

590

ISEE-3

15 MINUTE AVERAGE FLUXES + COUNT RATES
HOURLY AVERAGE FLUXES AND COUNT RATES

78-079A-12A, 78-079A-12B

Table of Contents

1. Introduction
2. Errata/Change Log
3. LINKS TO RELEVANT INFORMATION IN THE ONLINE NSSDC INFORMATION SYSTEM
4. Catalog Materials
 - a. Associated Documents
 - b. Core Catalog Materials

1. INTRODUCTION:

The documentation for this data set was originally on paper, kept in NSSDC's Data Set Catalogs (DSCs). The paper documentation in the Data Set Catalogs have been made into digital images, and then collected into a single PDF file for each Data Set Catalog. The inventory information in these DSCs is current as of July 1, 2004. This inventory information is now no longer maintained in the DSCs, but is now managed in the inventory part of the NSSDC information system. The information existing in the DSCs is now not needed for locating the data files, but we did not remove that inventory information.

The offline tape datasets have now been migrated from the original magnetic tape to Archival Information Packages (AIP's).

A prior restoration may have been done on data sets, if a requestor of this data set has questions; they should send an inquiry to the request office to see if additional information exists.

2. ERRATA/CHANGE LOG:

NOTE: Changes are made in a text box, and will show up that way when displayed on screen with a PDF reader.

When printing, special settings may be required to make the text box appear on the printed output.

Version	Date	Person	Page	Description of Change
01				
02				

3 LINKS TO RELEVANT INFORMATION IN THE ONLINE NSSDC
INFORMATION SYSTEM:

<http://nssdc.gsfc.nasa.gov/nmc/>

[NOTE: This link will take you to the main page of the NSSDC Master Catalog. There you will be able to perform searches to find additional information]

4. CATALOG MATERIALS:

- a. Associated Documents To find associated documents you will need to know the document ID number and then click here.
<http://nssdcftp.gsfc.nasa.gov/miscellaneous/documents/>

- b. Core Catalog Materials

ISEE 3

15-MIN AVG FLUX: H, HE + Z 2; TAPE

78-079A-12A SPHE-00318

THIS DATA SET HAS BEEN RESTORED. IT ORIGINALLY CONTAINED ONE 9-TRACK, 1600 BPI TAPE WRITTEN IN BINARY. THERE IS ONE RESTORED TAPE. THE DR TAPE IS A 3480 CARTRIDGE AND THE DS TAPE IS 9-TRACK, 6250 BPI. THE ORIGINAL TAPE WAS CREATED ON A PDP1 COMPUTER AND WAS RESTORED ON AN IBM 9021 COMPUTER. THE DR AND DS NUMBER ALONG WITH THE CORRESPONDING D NUMBER AND TIME SPAN IS AS FOLLOWS:

DR#	DS#	D#	FILES	TIME SPAN
DR004918	DS004918	D057301	1	08/13/78 - 12/01/78

ISEE 3

1-HR. AVG FLUX:H, HE &Z>2;TAPE

78-079A-12B SPHE-00349

THIS DATA SET HAS BEEN RESTORED. ORIGINALLY IT CONTAINED FOUR 9-TRACK, 1600 BPI TAPES WRITTEN IN BINARY. THERE IS ONE RESTORED TAPE. THE DR TAPE IS A 3480 CARTRIDGE AND THE DS TAPE IS 9-TRACK, 6250 BPI. THE ORIGINAL TAPES WERE CREATED ON PDP1 COMPUTER AND THEY WERE RESTORED ON AN IBM 9021 COMPUTER. THE DR AND DS NUMBERS ALONG WITH THE CORRESPONDING D NUMBERS AND THE TIME SPANS ARE AS FOLLOWS:

DR#	DS#	D#	FILES	TIME SPAN
DR004833	DS004833	D057302	1	12/01/78 - 01/01/79
		D057303	2	12/31/78 - 01/01/80
		D060473	3	01/06/80 - 01/04/81
		D063973	4	01/04/81 - 01/03/82

REQ. AGENT

DEW

DAD

RAND #

V0187

V0262

ACQ. AGENT

HKH

HKH

ISEE 3

15 MINUTE AVERAGE FLUXES AND COUNT RATE

HOURLY AVERAGE FLUXES AND COUNT RATE

78-079A-12A

78-079A-12B

This data set catalog consists of 5 tapes. One tape is for data set 78-079A-12A and four tapes are for data set 78-079A-12B. The tapes are 1600 BPI, 9 track, binary and contain on file of data. The tapes were created on a PDP1 computer. The D and C numbers along with the time spans are as follows:

78-079A-12A

<u>D#</u>	<u>C#</u>	<u>TIME SPAN</u>
D-57301	C-23126	08/13/78 - 12/01/78

78-079A-12B

<u>D#</u>	<u>C#</u>	<u>TIME SPAN</u>
D-57302	C-23127	12/01/78 - 01/01/79 12/31/78
D-57303	C-23128	12/31/78 - 01/01/80
D-60473	C-23662	01/06/80 - 01/04/81
D-63973	C-24098	01/04/81 - 01/03/82

PROGRESS REPORT

on the

CALTECH HEAVY ISOTOPE SPECTROMETER TELESCOPE (HIST) ON ISEE-3 (NASA Contract NAS5-20721)

1 July to 30 September 1982
1 October to 31 December 1982

Progress on HIST data analysis during the reporting period is described below. An updated HIST bibliography is also enclosed. The operation of the instrument during this period has remained unchanged.

Cosmic Ray Isotopes

During this period we completed work on two publications. The first, entitled "Samples of the Milky Way" was published in the December 1982 issue of Scientific American. Written in collaboration with M.E. Wiedenbeck of U.C. Berkeley, it focuses on the Caltech and Berkeley ISEE-3 measurements of the isotopic composition of cosmic ray Ne, Mg, and Si, and their interpretation.

A second article was completed as part of the U.S. Quadrennial Report to the IUGG (1979-1982). This article, to be published in Reviews of Geophysics and Space Physics, reviews recent progress in studying the elemental and isotopic composition of cosmic ray source material. It includes, in particular, recent ISEE-3 and HEAO-3 results.

Solar Flare Isotopes

J.D. Spalding has completed his Ph.D. thesis on the isotopic composition of solar flare nuclei. Work is beginning on an article for the Astrophysical Journal that will summarize his results.

NSSDC Submission

We have now completed production of the first two years of data (1978-1979) that we are submitting to the NSSDC. The data, which will be submitted on magnetic tape, include hourly average fluxes of H, He, and $Z \geq 3$ nuclei in several energy intervals. The documentation that will accompany this data submission is also essentially complete, with submission expected in early 1983.

SRL TECHNICAL REPORT 83-1

**DATA SUBMISSION TO THE NSSDC
FROM THE CALTECH HEAVY ISOTOPE SPECTROMETER TELESCOPE
ON ISEE-3**

R. A. Mewaldt

E. C. Stone

R. E. Vogt

California Institute of Technology

Pasadena, California 91125

February, 1983

Contents

I. Introduction.....3
II. Instrument Description.....3
III. History of Instrument Operation.....4
IV. Description of the Data.....5
V. Tape Format.....7
VI. Acknowledgements.....8
VII. HIST Bibliography.....22

I. Introduction

Caltech is furnishing data to the NSSDC from the Heavy Isotope Spectrometer Telescope (HIST) on ISEE-3. The data consist of counting rates and absolute fluxes for hydrogen and helium nuclei, and counting rates for $Z \geq 3$ nuclei, in several energy intervals. Other related data is also provided. The data are averaged over 1-hour time intervals, except for the first 3 and 1/2 months following launch, for which 15-minute averages are provided. This report describes the HIST experiment and the data provided. A bibliography is included for the reader who wishes additional information.

HIST is designed to measure the isotopic and elemental composition, and the energy spectra, of solar, galactic, and interplanetary cosmic-ray nuclei for the elements from H through Ni ($Z=1$ to $Z=28$) in the energy range from ~ 3 to ~ 250 MeV/nucleon. The results of these measurements are important to studies of the composition of solar matter and galactic cosmic-ray sources, the study of nucleosynthesis processes, studies of particle acceleration and propagation, and studies of the life history of cosmic rays in the heliosphere and in the galaxy. The principal investigator for the HIST experiment is E. C. Stone, with R. E. Vogt as co-investigator.

II. Instrument Description

A. The Telescope

The HIST instrument consists of a telescope of solid-state detectors and associated signal-processing electronics, as described in Althouse *et al.* (1977). The telescope consists of 11 silicon solid-state detectors of graduated thicknesses, as summarized in Table 1 and shown schematically in Figure 1. A unique feature of HIST is the use of position sensitive detectors, M1 and M2, which allow the determination of the trajectory of incident particles. M1 and M2 are 50 μm -thick surface-barrier devices with a matrix of strips forming an x-y hodoscope. There are 24 parallel "x" strips on one side of the detector, and, orthogonal to these, 24 "y" strips on the other side. The strips are spaced at 1 mm intervals. Each strip of M1 or M2 is connected to a charge-sensitive preamplifier, shaping amplifier, and threshold discriminator. In addition, signals from the strips of one side of each detector are summed and digitized by two 4095-channel analog to digital converters (ADCs).

Detectors D1, D2, and D3 are conventional surface-barrier detectors, while D4 to D9 are double-grooved Li-drifted detectors with a central area for measuring energy loss and an annular guard (G) used as an anticoincidence shield. Detectors D1, D2, D3, and the centers of D4 through D8 are each direct coupled to separate charge-sensitive preamplifiers, shaping amplifiers, and 4095-channel ADCs. The center of D9 and the guard regions of D4 through D9 are each connected to preamplifiers, shaping amplifiers, and discriminators. Each guard signal channel has two discriminators; G1 is sensitive to minimum ionizing particles, while G2 will trigger only on nuclei with more than 5 MeV energy loss.

The telescope is covered by two windows that protect the detectors from sunlight and provide an electrical shield. The outer window is a 6 μm -thick aluminum foil (1.40 mg/cm^2), while the inner window is 12.7 μm

aluminized-Mylar (1.6 mg/cm²).

B. Analysis Modes

For particles which stop in detectors M2 through D8, the residual energy E' is measured in the stopping detector, and the energy losses ΔE are measured in up to four preceding detectors (see Table 2). In this report we label the "Range" of an event by the identification of the last detector triggered. Thus, for example, particles stopping in M2 are labeled Range 0, while particles stopping in D1 are labeled Range 1, and so forth.

Because the telemetry rate is insufficient to transmit pulse-height-analysis (PHA) information for every event during periods of high count rates, a priority system selects a sample of the most interesting events for transmission. Highest priority is given to stopping particles with $Z \geq 3$, as identified by the pulse heights in the last two detectors triggered. For these "HiZ" events the priority system has a "rotating" feature that assures that each Range is equally represented in telemetry. For particles that penetrate D9, the energy losses ΔE are measured in D5 through D8; these particles and stopping particles with $Z < 3$ ("LoZ") are given lower priority. The requirements for these event types are summarized in Table 3.

HIST also accumulates "rate" data which is used to normalize particle fluxes and monitor instrument health. Rate accumulators are used to monitor events of various types during 64 second intervals, and to monitor individual detector count rates. Some of these rates are subcommutated, such that they are accumulated over 1 out of 8, or 1 out of 24 of the 64 second intervals. There are 16 rates which are counted separately in eight directional sectors of spacecraft rotation. These sectorized rates include stopping HiZ events summed over Ranges 0 to 8, and the instrument live time in each of the 8 sectors.

C. Orientation on the Spacecraft

The telescope acceptance direction (telescope axis) is oriented perpendicular to the spacecraft spin axis, which is approximately normal to the ecliptic, so that the instrument scans the particle fluxes in ecliptic as the spacecraft spins. The ecliptic plane is divided into 8 equal sectors and each event is tagged according to its sector of incidence.

III. History of Instrument Operation

A. Instrument Reconfiguration

ISEE-3 was launched on 8/12/78 into a heliocentric orbit 0.99 AU from the sun. HIST was turned on initially on 8/13/78. The experiment operated normally from 8/13/78 to 12/1/78, with element and isotope resolution for $1 \leq Z \leq 28$ nuclei consistent with its design specifications. On 12/1/78, after 110 days of operation, HIST experienced a component failure in its read-out logic, with the result that a portion of the data bits associated with each analyzed event were no longer transmitted to earth. In particular, one half of the PHA bits were no longer transmitted, and the hodoscope information was also degraded. The counting rate data was not affected by this failure. In order to limit

ambiguities in the interpretation of the event data, HIST was commanded into a reconfigured mode in which it functions as an element spectrometer (abundant elements with $1 < Z < 26$) having somewhat reduced geometry factor and energy coverage.

Table 4 summarizes the instrument's operation history. Note that during time periods 3 and 4 some of the M1 and M2 strips were commanded off, which has the effect of providing a clean, well-defined geometry, with somewhat reduced collecting power. Note also that following 79:053:1825 detectors D6, D7, and D8 were disabled by command. This reduced the energy coverage of the instrument, but does not affect any of the data submitted to the NSSDC.

B. HIST Geometry Factors

Table 5 summarizes HIST geometry factors for events with Range 0 through Range 4, as a function of the instrument's operation status (see Table 4). The geometry factors for Periods 1 and 2 are somewhat different from (and supersede) those in Althouse *et al.* (1977) because measured (rather than nominal) detector parameters were used in their calculation. Table 5 includes only those Ranges used for the NSSDC data submission; it is these values that were used in calculating the absolute fluxes that are being submitted from HIST.

It should be emphasized that the component failure on 12/1/78 affected only the data bits associated with individual pulse-height analyzed events; it did not affect the counting rate data (e.g., the LoZ and HiZ rates, see Section IV). Note, however, that the counting rate data are also governed by the geometry factors in Table 5, and that no corrections have been applied to these raw counting rate data to correct for changes in the instrument configuration.

IV. Description of the Data

The data submitted from HIST consists of time-averaged counting rates and absolute fluxes over several energy intervals. For the first 110 days following launch (Period 1 in Table 4) 15-minute averages are provided; for all subsequent time periods the quantities are averaged over 1-hour intervals.

A. Counting Rate Data

A total of 18 time-averaged counting rates are provided. Of these, 11 (the LoZ and HiZ rates) have a well-defined and generally useful physical interpretation, while the remaining 7 can be categorized as engineering rates. All rate data have been corrected for instrumental deadtime using HIST's built-in live-time monitor. The uncertainties given are statistical.

Table 6 summarizes the energy intervals over which the LoZ and HiZ rates respond. Note that the LoZ rates respond only to $Z=1$ and $Z=2$ nuclei (typically dominated by protons), while the HiZ rates respond only to $Z \geq 3$ nuclei (typically dominated by CNO nuclei). Table 6 also gives the coincidence requirements for each rate. Note that because they all require that both M1 and M2 trigger (300 keV thresholds for ~ 50 μm -thick detectors) these rates are extremely insensitive to electrons of all energies. However, this requirement also affects the proton

detection efficiency at energies greater than ~ 12 MeV. Thus the proton detection efficiency of the Range 4 LoZ rate (LoZ R4) varies from ~ 1 at 12 MeV to < 0.1 at ~ 20 MeV. The geometry factors appropriate to these rates are listed in Table 5. The user is again reminded that these geometry factors are not the same for all time periods (see Tables 4 and 5), and that no corrections have been applied to the counting rates for these changes. Figure 3 shows an example of some of the HIST rate data during a solar active period.

Table 6 also includes the duty cycle for the LoZ and HiZ rates. The LoZ rates by range were accumulated sequentially over every eighth 64-second interval (e.g., during the first 64-second interval HIST counted LoZ R0 events; during the second interval LoZ R1 events; and so forth). Thus the time intervals for the individual LoZ rates (by Range) do not coincide. The LOZSUM rate (see Table 10), which has a duty cycle of 1, sums over all Ranges that are operational (from 0 to 8), but is typically dominated by the first few Ranges. Note that (within the limitations of the statistics of small numbers) the LOZSUM rate should be somewhat greater, but approximately equal to, the sum of the LoZ rates from Ranges 0 to 4. Because of data gaps, it is possible that a particular LoZ rate (by Range) was not counted at all during a given time interval. For data to be reported from a given time interval, it was required that ≥ 8 minutes of data be available from the 15-minute time intervals (Period 1 in Table 4) and that ≥ 16 minutes of data be available from the 1-hour intervals (Periods 2,3, and 4).

The other counting rate data provided consist of single detector counting rates for M1, M2, and D1 through D5. These rates are primarily of engineering value. For example, if one of these detectors were to become noisy (as indicated by an increased and irregular counting rate during quiet times) this condition could lead to chance coincidences with normal events (relevant resolving time is a few microseconds) and thereby distort the Range distribution of LoZ and HiZ nuclei.

The user is warned that there are occasional bit errors on the HIST data tapes received by Caltech that may affect the counting rate data. Although the rate data were "filtered" to check for and discard obvious bit errors leading to impossible or inconsistent counting rates, no "trend checking" was done, and it is likely that some bit errors have gone undetected. These can only be identified by looking for isolated anomalies that deviate from the trend of the data.

B. Absolute Flux Data

The second type of data provided consists of absolute fluxes of hydrogen and helium nuclei in several energy intervals ranging from ~ 2 to ~ 20 MeV/nucleon. These fluxes were obtained using the PHA data to identify the relative abundances of H and He nuclei; the geometry factors in Table 5; and the LoZ counting rates to normalize the absolute fluxes. Table 7 summarizes the energy intervals for which absolute fluxes are provided; these intervals are determined by the various Ranges within HIST. Absolute fluxes for H nuclei with ~ 12 to ~ 20 MeV are not reported because protons in this energy interval are not fully efficient at triggering M1 and M2, as discussed above.

During Period 1 (see Table 4) H and He nuclei were identified in the conventional manner by counting the number of events within the appropriate regions of the two-dimensional PHA matrices formed from the

pulse heights of the last two triggered detectors. For data from subsequent Periods, similar methods were developed, using the available PHA bits from the last 2 (or in some cases 3) triggered detectors. These algorithms were found to give satisfactory resolution of H, He, and also heavier abundant elements. Figure 2 shows a comparison of the two methods, using data from the large solar flare that occurred on September 24, 1978 (during Period 1). The H and He points labeled HIST-I use the original element identification scheme and the full HIST geometry. The points labeled HIST-II use only those events within the 16x16 matrix of M1 and M2 strips that are active during Period 4 (see Tables 4 and 5). In addition, the HIST-II fluxes are based on the new element identification methods, and use only those PHA bits still available during Periods 2, 3, and 4. Thus the effect of the failure was simulated. As can be seen in Figure 2, the two methods are in good agreement. While there are small differences visible between the He fluxes derived from the two methods, the differences are in all cases <10% when the small changes in the energy intervals involved are taken into account.

Several intermediate quantities used in calculating the H and He fluxes are included on the tape so that the user can reproduce these values, or combine data over longer time intervals if desired. In particular, the number of events of each type and the instrument live time for LoZ events are provided for each time interval. Note that the live times can become very small during periods of high count rates because not all events that trigger the instrument can be telemetered. Also given is the "multiple hodoscope" (MH) event fraction, that is, the fraction of events that trigger 2 or more non-adjacent strips on either M1 or M2. During quiet times this fraction is very low (<1%), but it may increase dramatically during intense solar events due to the occurrence of chance coincidences of 2 or more particles. Such MH events are identified by HIST and tagged, but were not included in the flux calculation. Instead, these events were counted (by Range) and a correction factor applied to the H and He fluxes from each Range. Although summed over all Ranges, the MH event fraction on the tape should closely approximate the fraction for the individual Ranges.

V. Tape Format

This section describes the format of the HIST data on the magnetic tapes submitted to the NSSDC. These tapes contain small logical records called "Chapters" packed into long physical records. For the purposes of this report, a Chapter is defined by a "KEY" value stored in the first two-byte word of the chapter and a chapter length, specified in this document. The four different types of Chapters appearing on the tapes are listed in Table 8, and their format and contents described in Tables 9 through 12.

The physical record length varies but is always less than 8000 bytes. The first record on a tape contains ten Chapter 0's (i.e., Chapters with a KEY value of 0, see Table 9), each of which is 64 bytes long. Following the Chapter 0's in the first record are 28 Chapter 36's (described in Table 10) and finally a 4-byte Chapter 101 (Table 11) which flags the end of data in that physical record. Following records contain only the Chapter 36's and 101's until the last record, which has a string of 4-byte Chapter 103's (Table 12) which flag the logical end-of-tape. A

double end-of-file follows the last record.

It is our intention to submit one tape per year of data from HIST. We have, however, made an exception for 1978, where the first tape (HIST78.1) consists of 15-minute averages, and includes data obtained before the malfunction of the HIST readout logic; while the second tape (HIST78.2) consists of 1-hour average data obtained following this malfunction. In general, the time period covered by each tape will not start (or end) exactly at the beginning (or end) of the year (but should be within 1 or 2 days of this time), because the time boundaries were dictated by the boundaries of the experiment tapes received from the ISEE Project.

VI. Acknowledgements

A number of individuals made essential contributions to the data analysis task described in this report. The software necessary to produce the NSSDC tapes was written by N. Collins, B. Gauld, J. Kuyper, and S. Mjolsness, and the tape production was handled by R. Burrell. H. Breneman and J. Spalding made essential contributions to HIST data analysis procedures used here, while W. Althouse and M. Smith provided important consultation on the operation of the HIST instrument. We also thank T. Garrard for helpful advice. This work was supported in part by the National Aeronautics and Space Administration under Contract NAS5-20721 and Grant NGR 05-002-160.

Table 1 - HIST Telescope Characteristics

<u>Detector</u>	<u>Nominal Thickness</u> <u>(μm)</u>	<u>Nominal Area</u> <u>(mm^2)</u>	<u>Discrim. Threshold</u> <u>(MeV)</u>	<u>ADC Thresh.</u> <u>(MeV)</u>	<u>ADC Full Scale</u> <u>(GeV)</u>
M1	50	505	0.30	0.46	0.49
M2	50	505	0.30	0.46	0.49
D1	90	600	0.19	0.54	0.92
D2	150	800		0.71	1.2
D3	500	800		1.46	2.5
D4	1700	920 ¹		2.76	4.7
D5	3000	920 ¹		3.64	6.2
D6	3000	920 ¹		3.64	6.2
D7	6000	920 ¹		5.41	9.2
D8	6000	920 ¹		5.41	9.2
D9	3000	920 ¹	0.19	-	-

¹Area given is for central detection region.
In addition there is an annular guard
region of $\sim 450 \text{ mm}^2$ area (see text).

Table 2 - HIST "Ranges"

<u>Range</u>	<u>Last Detector Triggered</u>	<u>Coincidence Requirement¹</u>	<u>Pulse Heights Telemetered</u>
0	M2	$M \cdot \overline{D1} \dots \overline{D9}$	M1, M2
1	D1	$M \cdot D1 \cdot \overline{D2} \dots \overline{D9}$	M1, M2, D1
2	D2	$M \cdot D2 \cdot \overline{D3} \dots \overline{D9}$	M1, M2, D1, D2
3	D3	$M \cdot D3 \cdot \overline{D4} \dots \overline{D9}$	M1, M2, D1, D2, D3
4	D4	$M \cdot D4 \cdot \overline{D5} \dots \overline{D9}$	M1, D1, D2, D3, D4
5	D5	$M \cdot D5 \cdot \overline{D6} \dots \overline{D9}$	M1, D2, D3, D4, D5
6	D6	$M \cdot D6 \cdot \overline{D7} \dots \overline{D9}$	M1, D3, D4, D5, D6
7	D7	$M \cdot D7 \cdot \overline{D8} \cdot \overline{D9}$	M1, D4, D5, D6, D7
8	D8	$M \cdot D8 \cdot \overline{D9}$	M1, D5, D6, D7, D8
9	D9	$M \cdot D9$	M1, D5, D6, D7, D8

¹
Where M is defined as $M1X \cdot M1Y \cdot MZX \cdot MZY$

Table 3 HIST Event Types

<u>Coincidence Requirement</u>	<u>Description</u>
$M1X \cdot M1Y \cdot M2X \cdot M2Y \cdot Z3 \cdot \overline{D9} \cdot \overline{G2}$	Stopping, $Z \geq 3$
$M1X \cdot M1Y \cdot M2X \cdot M2Y \cdot \overline{Z3} \cdot \overline{D9} \cdot \overline{G1}$	Stopping, $Z < 3$
$M1X \cdot M1Y \cdot M2X \cdot M2Y \cdot D9 \cdot \overline{G2}$	Penetrating, $Z \geq 2$

M1X = logical OR of all M1X strip discriminators

Z3 = 1 for stopping particles with $Z \geq 3$

= 0 otherwise (computed from ADC pulse heights)

Table 4 - Summary of HIST Operation

<u>Time Period</u>	<u>Start</u>	<u>End</u>	<u>Comments</u>
1	Launch	78:335:2019	Normal Operation
2	78:335:2020	79:053:1824	Not all "event data bits transmitted after this time. "Rate" data unaffected.
3	79:053:1825	79:079:2232	Detectors D6, D7, D8, turned off. M1 reduced to 16 x 16 strips. M2 reduced to 8 x 8 strips.
4	79:079:2233	present	Detectors D6, D7, D8 turned off. Both M1 and M2 changed to 16 x 16 strip arrays.

Table 5 - HIST Geometry Factors (cm²sr)

<u>Last Detector Triggered</u> ¹	<u>Range</u>	<u>Time Period</u> ²		
		<u>1,2</u>	<u>3</u>	<u>4</u>
M2	0	0.79	0.063	0.25
D1	1	0.73	"	"
D2	2	0.73	"	"
D3	3	0.72	"	"
D4	4	0.70	"	"

¹ All previous detectors must also trigger

² Time periods defined in Table 4

Table 6 - Counting Rate Energy Intervals (in MeV/nucleon)

<u>Range</u>	LoZ		<u>Duty Cycle</u>	<u>HiZ¹</u>	<u>Duty Cycle</u>
	<u>¹H</u>	<u>⁴He</u>			
0	2.3 - 3.2	2.2 - 5.1	1/8	4.3 - 6.4	1
1	3.2 - 4.8	3.1 - 4.7	1/8	6.4 -10.0	1
2	4.8 - 6.9	4.7 - 6.6	"	10.0 -14.3	1
3	6.9 -11.8	6.6 -11.3	"	14.3 -24.6	1
4	11.8 -20.9 ²	11.3 -20.4	"	24.6 -45.6	1

¹ Energy intervals listed are for ¹⁶O.

² Proton efficiency < 100% and spectral dependent

Table 7 - Absolute Flux Energy Intervals¹

<u>Range</u>	Time Period 1		Time Period 2,3,4	
	<u>Hydrogen</u>	<u>Helium</u>	<u>Hydrogen</u>	<u>Helium</u>
0	2.3 - 3.2	2.2 - 3.1	2.3 - 3.2	2.3 - 3.1
1	3.2 - 4.8	3.1 - 4.7	3.2 - 4.8	3.2 - 4.7
2	4.8 - 6.9	4.7 - 6.6	4.8 - 6.9	4.7 - 6.6
3	6.9 - 11.8	6.6 - 11.3	6.9 - 11.8	6.8 - 11.0
4	_____	11.3 - 20.4	_____	11.3 - 20.4

¹ Energy intervals (in MeV/nucleon) are for ¹H and ⁴He, which dominate the H and He fluxes.

Table 8 - Index of Chapters

<u>Chapter Number</u>	<u>Chapter Name</u>	<u>Length (bytes)</u>	<u>Comments</u>
0	CNTRL	64	Header Information
36	HISTDC	276	Time, Status, and Data
101	EOR	4	Flags end of Physical tape record
103	EOT	4	Flags end of data on tape

Table 9 - Format and Contents of Chapter 0 (CNTRL)

<u>Item Name</u>	<u>Item Length (bytes)</u>	<u>Relative Index (bytes)</u>	<u>Date Type</u>	<u>Comments</u>
KEY	2	0	I	KEY = 0
Spare	2	2	A	Spare
PVRS	8	4	A	Program version date
EXDT	8	12	A	Execution date
TPNM	8	20	A	Tape name
Spare	4	28	—	Spare
CHNO	2	32	I	Irrelevant
CHLN	2	34	I	"
VPNT	12 x 2	58	I	"
VRCN	2	60	I	"
Spare	2	62	—	Spare
		64		

Table 10 - Format and Contents of Chapter 36 (HISTDC)

<u>Item Name</u>	<u>Item Length (bytes)</u>	<u>Relative Index (bytes)</u>	<u>Date Type</u>	<u>Comments</u>
^{KEY = 36} IYR	2	0	I	Year - 1900 (IYR ≥ 78)
IDY	2	2	I	Day of year (1 ≤ IDY ≤ 366)
IHR	2	4	I	Hour of day (see note 1)
ITIME	4	6	I	= IHR + 100 × IDY + 100,000 × IYR ²
IMODE	2	10	I	HIST operation mode (0-4) ³
HCNT	4 x 4	12	I	Number H events (Range 0 to 3) ⁴
HECNT	5 x 4	28	I	Number He events (Range 0 to 4) ⁴
LOZSUM	4	48	R	LoZ rate (summed over Ranges) ^{5,6,7}
LoZ	5 x 4	52	R	LoZ rates (Range 0 to Range 4) ^{5,6}
HIZ	5 x 4	72	R	HiZ rates (Range 0 to Range 4) ^{5,6}
M	2 x 4	92	R	M1, M2 single detector rates ⁵
D	5 x 4	100	R	D1 to D5 single detector rates ⁵
ULOZSUM	4	120	R	Uncertainty ⁸ in LOZSUM rate
ULOZ	5 x 4	124	R	Uncertainties ⁸ in LOZ rates
UHIZ	5 x 4	144	R	Uncertainties ⁸ in HIZ rates
UM	2 x 4	164	R	Uncertainties ⁸ in M rates
UD	5 x 4	172	R	Uncertainties ⁸ in D rates
HFLX	4 x 4	192	R	Flux ⁹ of Ranges 0 to 3 Hydrogen
HEFLX	5 x 4	208	R	Flux ⁹ of Ranges 0 to 4 Helium

(continued on next page)

Table 10 - continued

<u>Item Name</u>	<u>Item Length (bytes)</u>	<u>Relative Index (bytes)</u>	<u>Date Type</u>	<u>Comments</u>
UHFLX	4 x 4	228	R	Uncertainties ¹⁰ in HFLX
UHEFLX	5 x 4	244	R	Uncertainties ¹⁰ in HEFLX
LZLT	4	264	R	Live time for analyzed LoZ events in seconds
MHF	4	268	R	Multiple hodo scope event fraction ¹¹ (≤ 1.0)

272

Notes to Table 10:

- 1) For Period 1 (see Table 4), for which 15-minute averages are provided, $IHR = 10 + \text{hour} + IQH$, where IQH is the quarter hour ($0 \leq IQH \leq 3$).
- 2) For Period 1, $ITIME = (IHR/10) + 100 \times IDY + 100,000 \times IYR$.
- 3) $IMODE = 1$ to 4 corresponds to data from Time Periods 1 to 4 (see Section III and Tables 4 and 5). $IMODE = 0$ means insufficient data for this period.
- 4) See Tables 5 and 7 for energy intervals and geometry factors.
- 5) All rates (and uncertainties) in units of counts/sec.
- 6) See Tables 5 and 6 for energy intervals and geometry factors.
- 7) $LOZSUM$ is summed over all operational Ranges (see Table 4). It is typically dominated by protons in the first few Ranges.
- 8) All uncertainties are statistical, based on the square root of the number of counts. If there were no counts, the corresponding rate = 0.0 and the uncertainty is derived from an upper limit of 1.86 counts. If there was no data available for this rate, both the rate and uncertainty are set = 0.0.
- 9) All fluxes and uncertainties are in units of particles per $\text{cm}^2 \cdot \text{ster} \cdot \text{sec} \cdot \text{MeV/nucleon}$. They are based on the event counts in HCNT and HECNT. See also Tables 5 and 7.
- 10) Flux uncertainties are statistical, based on the square root of the number of analyzed events. If no events were analyzed the flux is set = 0.0 and the uncertainty is derived from an upper limit of 1.86 events.
- 11) See explanation of multiple hodoscope events in Section IV.

Table 11 - Format and Contents of Chapter 101 (EOR)

<u>Item Name</u>	<u>Item Length (bytes)</u>	<u>Relative Index (bytes)</u>	<u>Date Type</u>	<u>Comments</u>
KEY	2	0	I	KEY = 101
RECNO	2	2	I	Record Number

Note: This Chapter flags end of physical tape record

Table 12 - Format and Contents of Chapter 103 (EOT)

<u>Item Name</u>	<u>Item Length (bytes)</u>	<u>Relative Index (bytes)</u>	<u>Date Type</u>	<u>Comments</u>
KEY	2	0	I	KEY = 103
RECTOT	2	2	I	total records on tape
		4		

Figure Captions

Figure 1: A schematic drawing of the HIST telescope. M1, M2, and D1 through D9 are all solid-state detectors described in Section II. M1 and M2 are position-sensitive devices. The annular regions of D4 through D9 (shaded regions marked G) are "guard" regions used in anticoincidence. The trajectory of a typical Range 3 event is indicated.

Figure 2: Solar-flare energy-spectra for protons (p) and alpha-particles (α) averaged over the time period 1978:266:0000 to 1978:271:0540. The plotted fluxes were calculated using both the original geometry factor and nominal PHA data (HIST-I), and using the reduced geometry factor, the PHA data, and the slightly reduced energy intervals appropriate to Period 4 (HIST-II, see discussion in Sections III and IV).

Figure 3: An example of HIST counting rate data for a solar-active period in 1981. Shown are LoZ rates from Range 0 and Range 3 (upper 2 traces) and also HiZ rates from the same two ranges (lower 2 traces).

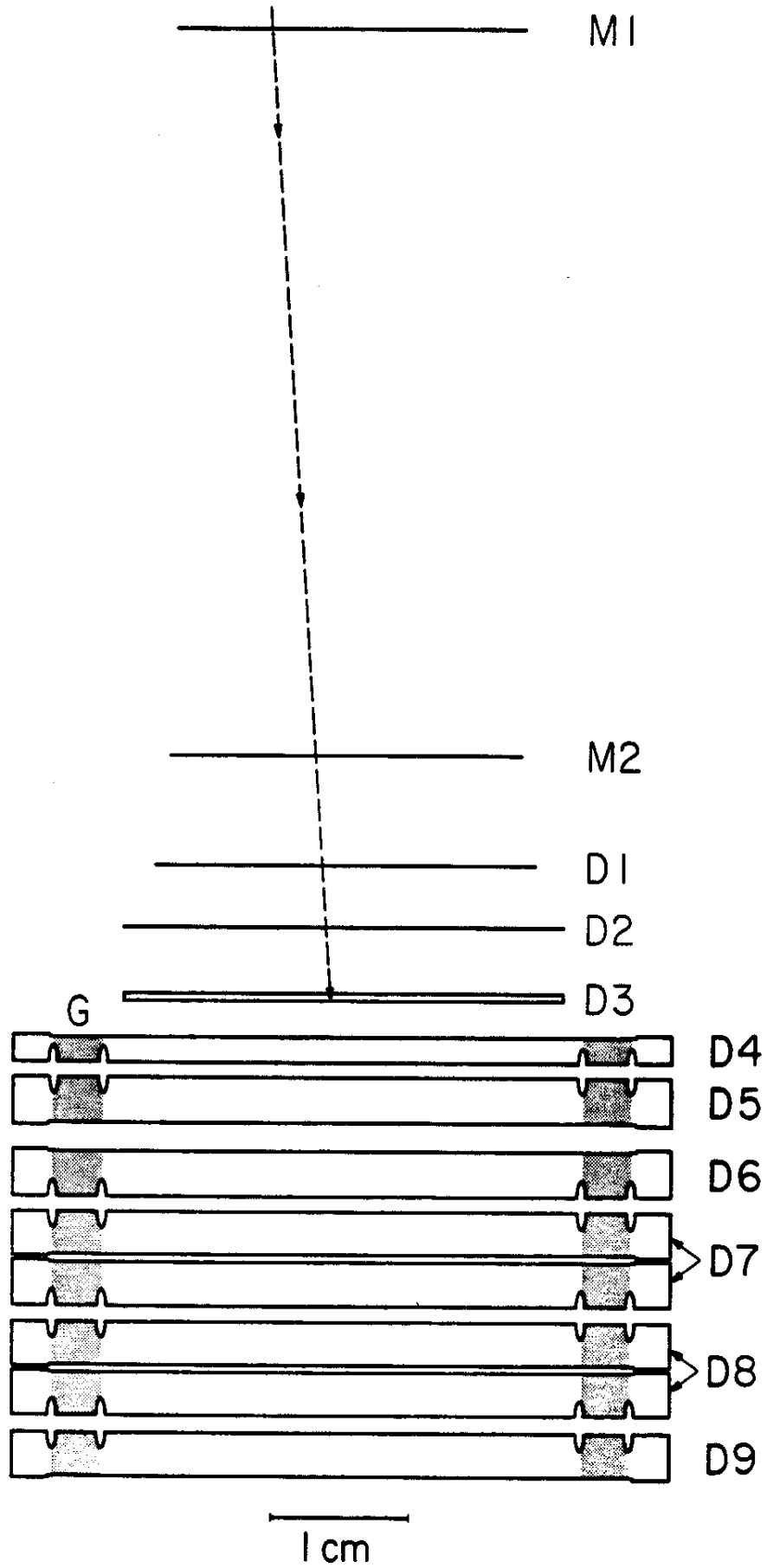


Fig. 1

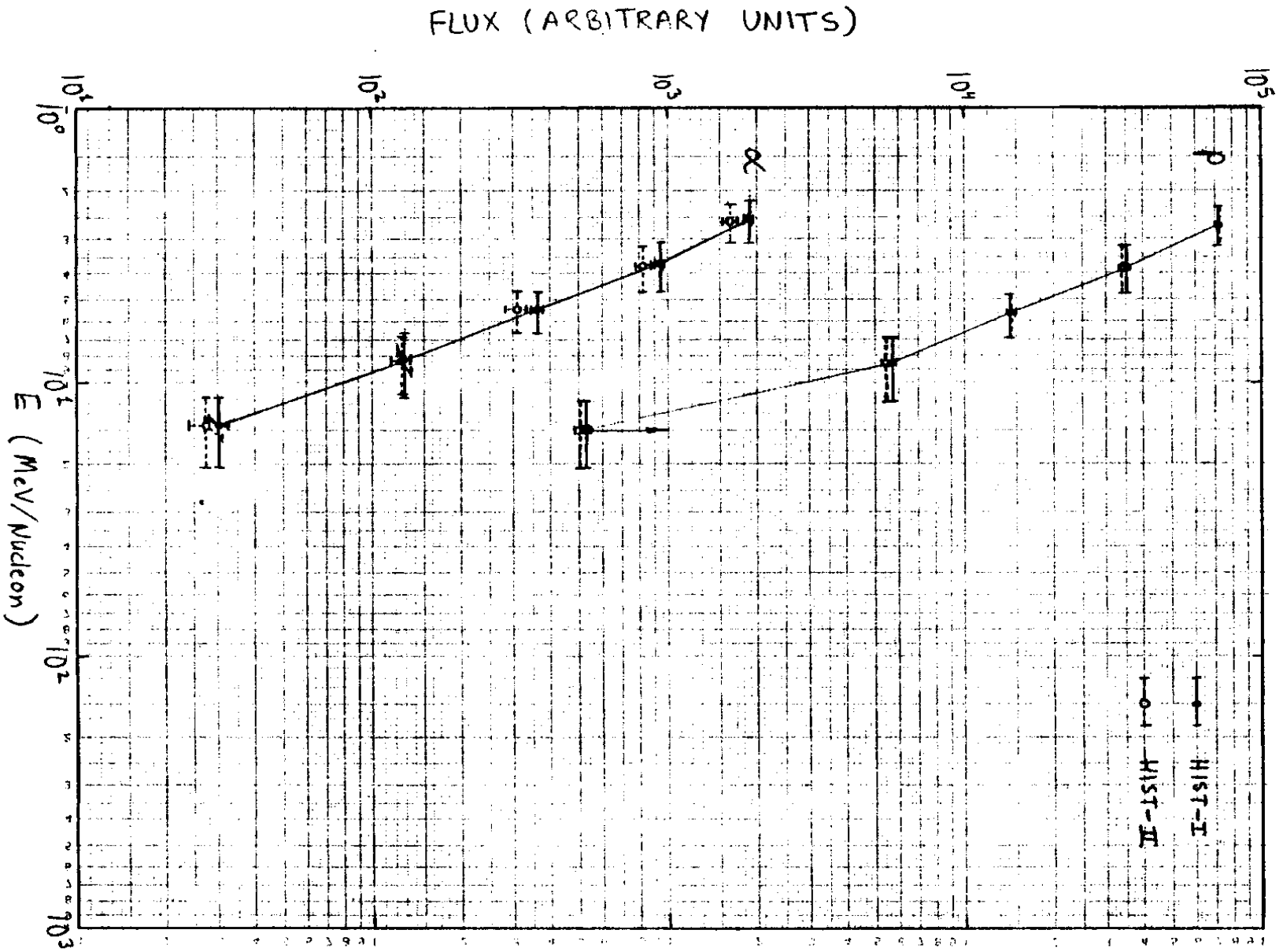


Fig. 2

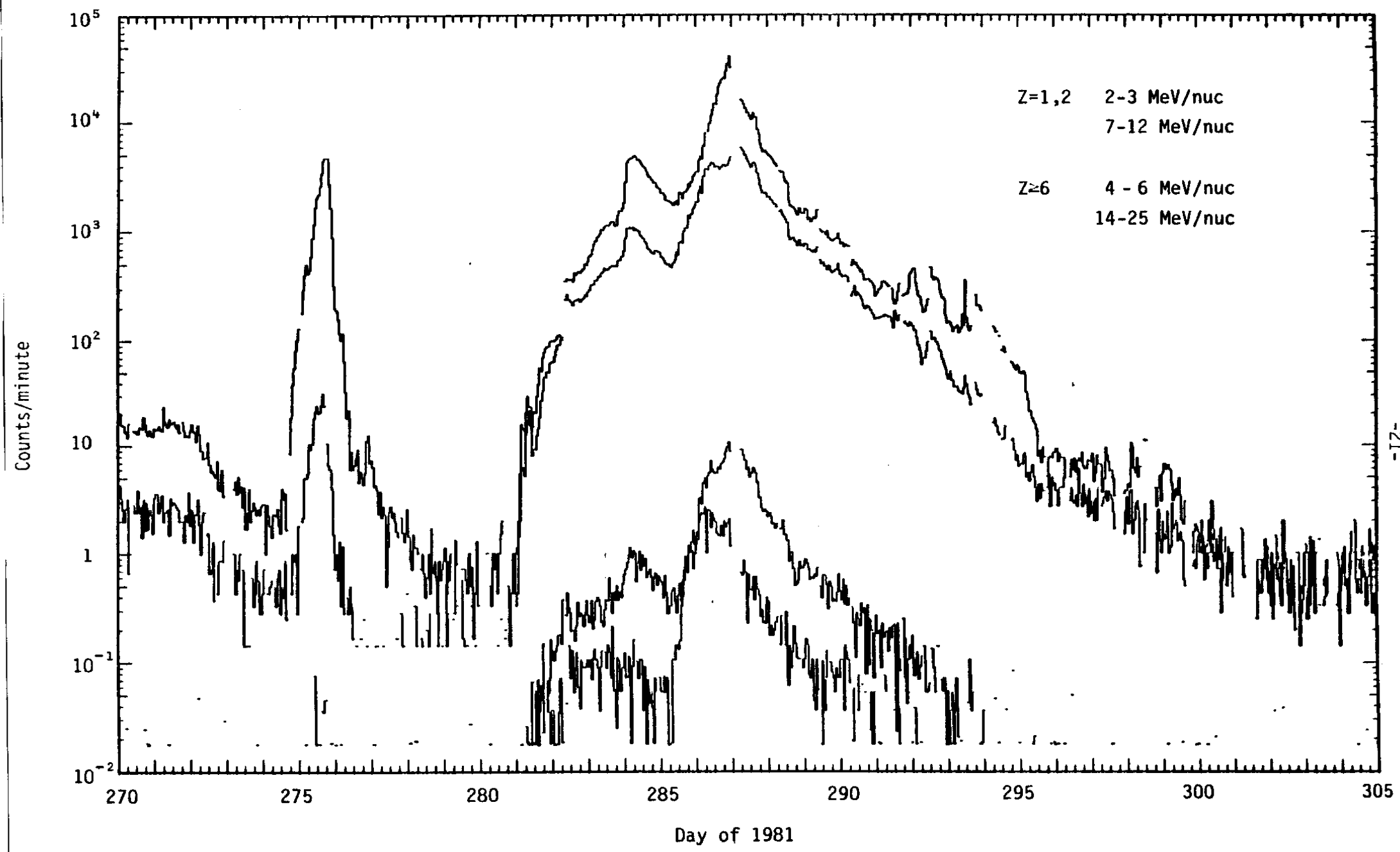


Fig. 3

VII. HIST Bibliography (12/31/82)

- Althouse, W.E., Cummings, A.C., Garrard, T.L., Mewaldt, R.A., Stone, E.C. and Vogt, R.E., A cosmic ray isotope spectrometer. IEEE Trans. on Geosci. Electron. GE-16, 204 (1978).
- Mewaldt, R.A., Spalding, J.D., Stone, E.C. and Vogt, R.E., The isotopic composition of solar flare accelerated neon. Ap.J. (Letters) 231, L97 (1979).
- Mewaldt, R.A., Spalding, J.D., Stone, E.C. and Vogt, R.E., Satellite measurements of the isotopic composition of galactic cosmic rays. Proc. 16th Intern. Cosmic Ray Conf., Kyoto, 12, 86 (1979).
- Mewaldt, R.A., Spalding, J.D., Stone, E.C. and Vogt, R.E., High-resolution measurements of galactic cosmic-ray neon, magnesium, and silicon isotopes. Ap.J. (Letters) 235, L95 (1980).
- Mewaldt, R.A., Spalding, J.D., Stone, E.C. and Vogt, R.E., The isotopic composition of galactic cosmic ray iron nuclei. Ap.J. (Letters) 236, L121 (1980).
- Mewaldt, R.A., Spacecraft measurements of the elemental and isotopic composition of solar energetic particles. Proc. Conf. Ancient Sun, ed. R.O. Pepin, J.A. Eddy, and R.B. Merrill (New York: Pergamon), p. 81 (1980).
- Mewaldt, R.A., Spalding, J.D., Stone, E.C. and Vogt, R.E., The isotopic composition of solar flare accelerated magnesium. Ap.J. (Letters) 243, L163 (1981).
- Mewaldt, R.A., Spalding, J.D., Stone, E.C. and Vogt, R.E., High resolution measurements of solar flare isotopes. Proc. 17th Intern. Cosmic Ray Conf., Paris, 3, 131 (1981).
- Mewaldt, R.A., Spalding, J.D., Stone, E.C. and Vogt, R.E., The isotopic composition of low energy cosmic rays. Proc. 17th Intern. Cosmic Ray Conf., Paris, 2, 68 (1981) and 11, 431 (1981).
- Mewaldt, R.A., Spalding, J.D., Stone, E.C. and Vogt, R.E., The isotopic composition of cosmic ray B, C, N, and O nuclei. Ap.J. (Letters), 251, L27 (1981).

- Mewaldt, R.A., The elemental and isotopic composition of galactic cosmic rays. Proc. 17th Intern. Cosmic Ray Conf., Paris, 13, 49 (1981).
- Mewaldt, R.A., Stone, E.C., and Wiedenbeck, M.E., Samples of the Milky Way. Scientific American 247, 100 (1982).
- Spalding, J., The isotopic composition of energetic particles emitted from a large solar flare. Ph.D. Thesis, CIT (1982).
- Mewaldt, R.A., The elemental and isotopic composition of galactic cosmic ray nuclei. To be published in Reviews of Geophys. & Space Phys. (1983).

(7560)	8640A8CC	94403240	36417AE1	6F41EFB0	723B99FF	883CB646	123C5888	883CB646	883CB646	883CB646
(7600)	083EB646	083EB646	083EB646	083EB646	083EB646	843D94EE	A93DEF9C	E73D9EB0	463E66C2	503EC270
(7640)	A33E93B3	8B3E2969	813C2E52	AE3CF221	000C0000	7A3A1FDF	0000C000	00000000	00000000	00000000
(7680)	00000000	153C6053	033CC3A1	893BF728	7A3A1FDF	253CDA64	E13BRD64	923B6E11	083BFFB8	793A695A
(7720)	544ECDC	00000000	65000100							

FILE	1	RECORD	263	LENGTH	4420	BYTES						
(0)	24000000	52000200	07007D00	0F200400	0000C205	00004B02	00009900	0C002700	00001700	00003000		
(40)	00000100	00000000	00000000	984022C8	4140144A	BA3FEFFA	9C3E0E02	923DC2D4	123CC2D4	00000000		
(80)	00000000	00000000	00000000	00000000	614453ED	E4410650	06417A36	DE403ECC	B140A3CD	444110BB		
(120)	6C417DB0	953DE1C6	283E5E77	EA3DA553	563C900A	CF3C88AE	123CC2D4	0E3B8C8D	083B8C8C	083B8C8D		
(160)	083B8C8D	083B8C8D	004090AE	A23E82B6	8C3E5761	7B3E4127	643E0981	A93E99F5	BA3EFDD5	5B41D847		
(200)	4940CC9D	1B3F63BF	873DB80F	613E3BDC	A03CCFDB	8A3BD7C2	00000000	00000000	B63EC1C4	053E7657		
(240)	453C9276	2D3C6304	3C3D68E6	393C59BE	8A3BD7C2	713E299E	CC3A3F4C	FC45CFDD	E33A89F3	24005354		
(280)	52000200	08007D00	10200400	0000B304	00000C02	0000B800	00001E01	00001300	00000B00	00000A00		
(320)	00002000	00001A00	8440CEFF	294080C7	AE3F305E	F33E8732	633F1D23	9C3E6F03	923A0ED6	003C4C7B		
(360)	123E0ED6	00000000	00000000	5E44E767	E44162EB	9B41D314	9F4183AB	8E41239B	9C410AF2	8D415607		
(400)	A33C6902	1D3E3CE4	E23D2A4A	853D779F	B63D0AA0	563D730C	923A0ED6	423BF73E	CF3A5DA8	083BC08E		
(440)	083BC08E	FF3F0591	B73E0F37	D53E8568	D83EE08A	CC3E08A5	D63EE4AF	CB3E7E82	4B41880E	4C40B7C1		
(480)	543FE7E8	0C3FB35B	533E6DB2	A73D1482	443DEEA3	933D583F	DA3C0532	BB3E7E57	0F3E0E1E	7A3D0978		
(520)	043CFACA	423C3774	CA3CB805	783CE98B	503C443D	AE3BA32A	E445497E	A33BADA2	24000000	52000200		
(560)	09007D00	11200400	0000FD02	00002B02	00008D01	00007501	00001C00	00001A00	0000230C	00001400		
(600)	00000A00	4C4178DC	5D40BB2D	8740685B	2C40BCE1	1C40BCC0	963E5219	673C590E	7C3BA70F	A83B6F0A		
(640)	A83A6F0A	00000000	81445AF4	7B42B90C	3A42569E	1C421A92	C5419C13	9341EDC0	774182C3	033E4D32		
(680)	423E54C3	573E197F	1F3E93EF	243E5001	623D9FED	8B3B0D55	113BCE87	283B6F0A	A83A6F0A	1C3B2547		
(720)	15409C4E	0C3FCCFB	323FD8EB	1D3FD57A	F03ED2BC	E13EFB25	CE3EDC28	9A415E0B	01416766	8840DEF5		
(760)	DA3FIDE3	3B3F2A12	EC3E1C3D	CD3EA5BD	DC3DAC16	C83C8EB2	333FE329	AF3E66C4	5B3E8DF6	B53D3656		
(800)	0D3E9069	B93D2652	8B3D2E1B	C43C6BDA	FD3B4ECD	314568AE	E63BCE74	24000000	52000200	0C007D00		
(840)	15200400	00005204	00009102	00001501	0000C800	00002300	00002300	0C000A00	00000A00	00000400		
(880)	26416CC8	A7402749	4B40BF03	9B3F638D	613F5A48	963D3C30	00000000	00000000	00000000	00000000		
(920)	00000000	A444AB6F	4342D531	C84159CF	8441F3C6	3E41A138	6441C04C	774155E9	EF3D7947	6F3EC0A3		
(960)	3B3E6B0B	E73D2A15	C43D8EA4	E33C4410	1F3BFBA0	1F3BFBA0	1F3BFBA0	1F3BFBA0	1F3BFBA0	28405C00		
(1000)	013FFF1D	033F2847	D53EFA8B	B23EA94D	C53E89F4	CE3E5548	AD415E94	ED4030CF	1440F79B	393F2841		
(1040)	353F0B4C	F63E4DDA	B63D16D4	2B3D8E21	F93B7EAF	273F5E05	943EF971	E03E71DD	503D8309	F53D8A28		
(1080)	AE3C25E7	E73C0243	583C3177	793B7EAF	64453C83	CC3AA71A	24000000	52000200	0E007D00	16200400		
(1120)	0000F004	00000603	00001A01	0000E700	00003800	00002900	00001700	0C000E00	00000100	09413951		
(1160)	874021DB	16401A81	783FE628	283FF2E2	A53D9970	583B6DB7	103B497A	903A497A	00000000	00000000		
(1200)	8D442E50	24420394	AB419DC4	6D41CE3E	2941792C	5541F443	78412204	C73DDE31	473EAE44	143E5FC5		
(1240)	BF3C9208	533D8E6A	DC3C2296	FA3A203E	CC3A8252	903A497A	063B3F5D	063B3F5D	1040242E	DC3EE202		
(1280)	E03E7ACE	BA3F07C9	9D3E818A	A73EE133	BE3E6AFA	8C41C4CC	C740F849	D83F2B8D	153FF869	4C3F48E2		
(1320)	CD3EFFB2	163E0079	293D5ACF	B03A52F8	FD3EA575	653EB639	CE3DC453	1C3D9D4A	DC3D6319	803DD07F		
(1360)	FB3C7801	353CD588	B03A52F8	A1450C34	553CE929	24001C47	5200C200	0F007C00	17200400	0000BA03		
(1400)	00004102	00001101	0000B600	00003200	00001300	00000900	0000CA00	00000100	0E412456	7F40DAE8		
(1440)	1040E8B3	5A3F79A9	173F5022	AB3DE77F	B63BD4EE	00000000	00000000	B63AD4EE	00000000	864418E0		
(1480)	1C4260FD	9F41281B	5F415F1E	1B41C35A	84416FC6	8141BD8B	DC3D8DDE	513EDE7E	2C3E7391	D43D2022		
(1520)	B03D7F5C	F23C7E89	363BD4EE	2A3BAB20	2A3BAB20	E63AD4EE	2A3BAB20	1E401F1E	F23E625E	E93EF59B		
(1560)	D63E6E44	B23C8ECE	CB3E9545	D23E46CB	87419E3A	BC40A42E	0340B9BF	153F7667	693FF8EB	713E867C		
(1600)	943DC003	193D42F0	E03A0D99	0C3F361A	7A3E2CB1	FF3D6E29	313D7331	043E7D53	5D3D679A	C53C555A		
(1640)	423CF2B7	E03A0D99	7E45B408	393CF98D	24009647	E2000200	10007D00	1E200400	00007C01	0000D700		
(1680)	00005100	00003A00	00001600	00000600	00000300	00000300	00000000	EC40FE51	E140A084	D43FF5D9		
(1720)	843FB687	203F7FA4	00000000	00000000	803B9983	00000000	00000000	00000000	7544E3FB	0942DA8C		
(1760)	7F41A785	384142C0	0841D38B	3E4157C3	644169EA	2E3E7245	B63E7374	693E2CE6	383E7390	0F3EDEAE		
(1800)	6F3C4009	EF3B4009	803B9983	EF3B4009	EF3B4009	EF3B4009	7B40C572	3C3FFC06	353F8C3E	1B3F7F55		
(1840)	043F2178	1C3F3493	2B3FF384	80413819	A840C40B	EA3F59C7	E33EEC92	743FB9C5	363E24C2	6B3DC1D2		
(1880)	DC3C3BBC	00000000	523F3748	B73EC75E	263EC114	6F3D2C0E	503E198E	953D8938	083D1227	7E3C16E2		
(1920)	F93B9E98	D444C497	A63B80F8	24C03B7B	52000200	110C7D00	1920C400	0C000605	0C00CE02	00002601		
(1960)	0000CF00	00003800	00001F00	00001400	00000B00	00000700	E0405104	7E4060F4	16403BDC	473F619F		
(2000)	F73EADCC	403D32BD	103BC245	00000000	00000000	00000000	00000000	6A441666	0242F45F	8541FD4B		
(2040)	3F41ECE0	124194B4	3E41CC71	7141DC4C	B33DB3C6	3F3E0834	143ECBD7	AE3DDC36	863DA4E3	9D3CEA5E		
(2080)	CC3A3908	063B652C	063B652C	063B652C	063B652C	FC3F437B	C33E2BAE	C53E67DC	A73E48DC	923EEEC6		
(2120)	A73E663B	B03E5115	7141D2E8	9E40AFF9	BD3F0CAD	E23E4D72	2D3FF8D6	833E4E38	CB3DB40B	E13C8BA7		
(2160)	023C4CF2	D73E74DD	3A3E3445	B03D78FE	FB3C6FD3	B93DB0D7	3C3DD18A	C43CADA5	083C2413	453BF3F8		
(2200)	BE45EEA0	933B8C53	24008247	52000200	12007D00	1A20FFFF	00001C01	0C00B000	0C003E0C	00002A00		
(2240)	00000700	00000A00	00000500	00000200	00000000	C24009A1	444032BB	1240718B	E03FF0DE	503FA8C6		
(2280)	00000000	00000000	00000000	00000000	00000000	00000000	6344FAAD	0342E03C	88416A01	2A415DA2		
(2320)	0141357B	3A41A5B1	7941D1ED	363ECE7F	9E3E9CFB	893ECD36	703E065C	673EBE9D	EE3DDDF7	133CB00E		

(2360)	133CB00E	133CB00E	133CB00E	133CB00E	8B4081A5	543F720B	3A3F26F1	143F2410	363F2E67	5B3F6706
(2400)	7D3FED6A	904129CB	9040DE57	963F68DF	463E5A68	133E3A23	963DE339	2C3CADD2	00000000	00000000
(2440)	EA3E42B2	313EA6EA	9C3D5679	A53CC07B	293D5FE6	C83C2E4D	F43B9768	963B3071	093BF42F	C145D164
(2480)	FE3BC149	24CCB646	52000200	13007D00	1B2C04C0	CC0CAE03	00003702	0C00DFC0	00007F00	00003200
(2520)	0C0C1FC0	000C0D00	00000B00	00000300	C340AB56	3E40C1B9	EA3F7439	3E3FE483	E63E8B35	003D247D
(2560)	00000000	00000000	00000000	00000000	00000000	56448B50	F041CA52	724198E0	274145A3	FF404E79
(2600)	3A41D8B5	7C41E275	8D3D140E	343E03C3	0D3E47A5	B13D7EE2	8C3D206D	943CBA5D	293BA9F2	293BA9F2
(2640)	293BA9F2	293BA9F2	293BA9F2	0740F57D	C33E52EE	CC3EE000	A93EC677	943E7913	E23E50D9	CF3E15F8
(2680)	4E416000	8E4015D3	A73F5337	A13E834F	343F4271	5E3ED427	A63D1E19	033D81C0	823BE851	D63ECEC7
(2720)	3F3E2AF0	B33D7229	E53C2506	CC3D8525	5A3DA39F	B83CE844	1D3C8CFE	163B037B	A445702E	C33B1AEC
(2760)	2400B646	52000200	14007C00	1C200400	0000EAC4	0C008D02	00001601	00009C00	00002F00	00001500
(2800)	0C0C0E00	0C0C0700	0000C030	B84084A7	424CE170	CC3FBEC7	273FA97B	C33E1413	923C9FDE	00000000
(2840)	00000000	00000000	00000000	00000000	4C4441D6	DB414ED2	59418C3D	1E418EB9	F040380A	3D41A922
(2880)	7A415ECB	A43D83A9	283E25F8	F73DF79C	9C3D8BD1	783D4DF8	4F3CC0A7	083B598E	083B598E	083B598E
(2920)	083B598E	083B598E	F53F7C43	E33EB7A8	E23EE799	973EDD36	843E7CC0	A63EEBA5	BF3E2AE6	52418A86
(2960)	7C4CE16D	9F3F110D	983EF28C	013D89CC	1E3E222E	883DC37A	803C94E5	473B76B3	BD3E6CF0	1E3E980D
(3000)	983DC2A0	C33CA4A9	973D0B77	0A3F2D12	913C1BE7	C23B824E	E63A4A98	D6450C48	9F3BEF00	24001C47
(3040)	52000200	150C7D00	1D200400	0000F404	00006602	0000E100	0C007800	00003200	00001800	00001300
(3080)	0C0C0100	0C0C0300	9F40FF0D	4F40E204	A13F3AB7	E63EC1F8	853EFC0A	123C47CE	903AFC3A	903AF03A
(3120)	00000000	00000000	00000000	3744F3EF	BD418E2B	344185C8	0B41817E	C140E9E2	374140CB	6D41FEB2
(3160)	973D1176	2E3EF454	D93D1AE7	833DE40C	453D80A4	123C47CE	903AF03A	903AF03A	063B5522	063B5522
(3200)	063B5522	E83F6464	A63EAAA5	A23E3EE9	8F3E701A	783E743E	A43E1443	BA3EBCCD	3F4123CE	56407160
(3240)	683F32E0	533E2144	F93E709C	233E1847	A73DB689	043BD80E	343B66A2	AC3EEB5A	0A3EB66C	783D9C66
(3280)	9A3C7749	8D3D8C33	053DD150	993CA0BE	043BD80E	D03A1F94	EC4551E6	00000000	24001C47	52000200
(3320)	160C7D00	1E2C0400	00007D04	00005302	0000D600	0C006300	00002A00	00001400	00000700	00000400
(3360)	0C0C0000	8740E07A	1440B586	A43F7702	003F8174	373EDD81	5C3D6F35	0C000000	00000000	00000000
(3400)	00000000	00000000	2344A96F	A3410282	1941428B	FC40779B	DD400C5B	3E413C88	6D4103B3	8D3D7D07
(3440)	133EDCA9	DB3D5A71	893D0353	243D4722	B33CB8CC	083B8887	083B8887	083B8887	083B8887	083B8887
(3480)	DB3F0E0F	9A3E93EE	963E1923	883E812B	7E3EBCEB	A73EFB3E	BA3EC2CC	2041ACBA	40404E20	4D3F5CC3
(3520)	213E3231	C13E4EE9	FB3D28AC	E53CC55D	F43BE742	00000000	973E11BC	FC3D7A0B	E13D040C	813C779A
(3560)	6F3D8F5E	E13C4B1A	2D3C7562	743BE742	CF3A0F26	0046F513	F13A0188	24009B7F	52000200	17007D00
(3600)	1F2C0400	00009303	0000D801	0000BA00	00006400	00001A00	00000D00	00001000	00000600	00000200
(3640)	7E4CECAF	02400476	8D3FA3E5	CB3E2C71	4E3EA6E2	A53C9545	2E3B7CEA	2E3B7CEA	0C0C0000	00000000
(3680)	00000000	19441460	9B417C4C	0E41A579	FC407F39	C3404614	4141C12E	7341255C	953D073F	153EE77A
(3720)	DC3D426B	893D9A15	3A3DA2A3	723C0A37	F73A575E	F73A575E	223BFDAB	223BFDAB	223BFDAB	E53F0E36
(3760)	A33E0217	973E2AC3	923EB8F7	863E6772	B53ECBE5	CC3E9628	1441CFC2	3C40F8F2	4E3F95B4	3D3E5B09
(3800)	863EDE83	BD3D3EED	973DC97C	543C62B1	013B634D	9C3E645F	023EDE50	723D8360	973CAF3A	5A3CA9E3
(3840)	D23C6DB4	973CC97C	AD3BBCA9	B63A6DDC	DC45A5A1	153BE548	24004446	15200130	00007D00	6C20FFFF
(3880)	000CC300	000C5E00	00001D00	00001100	00000600	00000500	00000000	00000200	00000000	36404BD3
(3920)	F03F08C9	203FB090	003EC073	803EC073	003CC073	000C0000	00000000	BA3BE9C6	0C0C0000	00000000
(3960)	DB43399B	484193B7	E04090CA	E04090CA	BA4033A8	4041A0AD	6E4139D7	023E45B0	AF3EEEE3	4B3EC619
(4000)	B53DA5A8	B53DA5A8	003DC073	2D3CBFC2	2D3CBFC2	BA3BE9D6	2D3CBFC2	2D3CBFC2	414015F0	213FD3C3
(4040)	293F1DEC	293F1DED	1A3FEDD7	1C3F3452	2F3FEC27	85412EB3	92402E42	5E3FBE18	0D3EBAB9	A43E2B88
(4080)	A23C6845	000C0000	00000000	00000000	303F8B23	8E3ED099	D03D1204	DA3C5F33	C63D7372	223D6845
(4120)	C33C8399	373CC615	A63B4EF4	1E45ADE9	453C9298	24003E47	52000300	01007D00	6D2C0400	0000A103
(4160)	000CCD01	000CA100	0000E000	000C1600	000C0C00	00000700	00000400	00000400	324002CD	C53FE942
(4200)	373FBB7F	9B3E5FF9	003E0373	DC3CE132	00000000	00000000	00000000	0C000000	00000000	D843950A
(4240)	63411554	CB40B491	E04045C9	CF404C95	314170E8	7E41D5EC	633DDEB1	F03D18A8	A43D5F20	553DA5FE
(4280)	093D6B51	7E3C7B43	063BC920	063BC920	063BC920	063BC920	063BC920	B23F1016	793E4996	743E5B79
(4320)	8C3E0373	763E62DF	A13E549B	C03E8B3C	C6405149	FD3FBDF9	FE3EAC1D	0C3EE5DE	273EA47C	783DCCFE
(4360)	BC3CDF41	C93EC562	373B7FA4	603EEDF9	BA3D53CF	2C3D9537	523CE771	0E3D53D5	8F3CECC1	0E3C254F
(4400)	493BC562	B73A7FA4	1B469758	00000000	65000601					

FILE	1	RECORD	264	LENGTH	400	BYTES				
(0)	67000701	67000701	67000701	67000701	67000701	67000701	67000701	67000701	67000701	67000701
(40)	67000701	67000701	67000701	67000701	67000701	67000701	67000701	67000701	67000701	67000701
(80)	67000701	67000701	67000701	67000701	67000701	67000701	67000701	67000701	67000701	67000701
(120)	67000701	67000701	67000701	67000701	67000701	67000701	67000701	67000701	67000701	67000701
(160)	67000701	67000701	67000701	67000701	67000701	67000701	67000701	67000701	67000701	67000701
(200)	67000701	67000701	67000701	67000701	67000701	67000701	67000701	67000701	67000701	67000701
(240)	67000701	67000701	67000701	67000701	67000701	67000701	67000701	67000701	67000701	67000701
(280)	67000701	67000701	67000701	67000701	67000701	67000701	67000701	67000701	67000701	67000701
(320)	67000701	67000701	67000701	67000701	67000701	67000701	67000701	67000701	67000701	67000701
(360)	67000701	67000701	67000701	67000701	67000701	67000701	67000701	67000701	67000701	67000701